

Fusion Cross Section Measurements for Systems ${}^6\text{Li} + {}^{27}\text{Al}$, ${}^{64}\text{Zn}$ at Near-Barrier Energies

M.D. Rodríguez^{*1}, I. Padron², G.V. Martí¹, R.M. Anjos², P.R.S. Gomes², J. Lubian², R.S.L. Veiga², A.J. Pacheco¹, O.A. Capurro¹, J.O. Fernández Niello¹, J.E. Testoni¹, A. Arazi¹, and M. Ramírez¹

¹Laboratorio Tandar, Departamento de Física, Comisión Nac. de Energía Atómica, Av. del Libertador 8250, (1419), Buenos Aires, Argentina

^{*}Departamento de Física, FECyN, UBA, Buenos Aires Argentina

²Instituto de Física, Universidade Federal Fluminense, Av. Litorânea, s/n, Niterói, R.J., Brasil

Received on 6 October, 2003

Fusion cross-sections were measured for the ${}^6\text{Li} + {}^{27}\text{Al}$, ${}^{64}\text{Zn}$ and ${}^9\text{Be} + {}^{64}\text{Zn}$ systems at energies around the Coulomb barrier, in order to study the influence of the break-up of weakly bound nuclei on the fusion process.

1 Introduction

The influence of the break-up of stable and radioactive nuclei on the fusion process at energies above and below the Coulomb barrier has renewed interest in the last years. Recently we have studied fusion cross sections at energies above the Coulomb barrier for the ${}^6\text{Li} + {}^{27}\text{Al}$ and ${}^6\text{Li} + {}^{64}\text{Zn}$ systems[1]. In this work, results obtained in two recent experiments are presented. They are the natural continuation of previous measurements, i.e. fusion cross-sections at low energies close to the Coulomb barrier, for the same systems mentioned above.

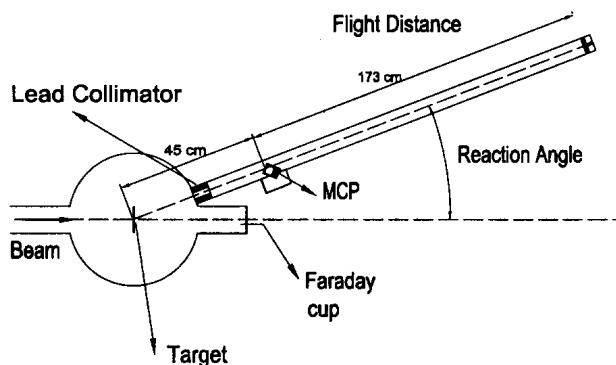


Figure 1. Schematic view of the experimental setup of the time of flight device used in the present work.

The experiments were performed at the 20-UD tandem accelerator of the TANDAR Laboratory, at Buenos Aires. Beams of ${}^6\text{Li}$ and ${}^9\text{Be}$ were provided by the TANDAR accelerator with energies ranging from 14 to 24 MeV. The detector system was a time of flight (TOF) consisting of a zero-time detector (Micro Channel Plate (MCP) [3 stages Burle MCP]) used as a start detector and a passivated implanted planar silicon (PIPS) detector [Canberra TMPD900-27-300] as the stop detector. The total FWHM resolution for the sys-

tem was 750 ps for a typical time of flight of 400 ns. A schematic view of the set-up is shown in Fig. 1.

The lead collimator placed at the entrance of the TOF line was set in order to shield the MCP from the intense x-rays produced when the beam impinges on the target. The reaction products at different scattering angles were detected taking advantage of a sliding flange between the scattering chamber and the TOF line, allowing angular distribution measurements at a reasonably wide angular range, and with angular uncertainties of 0.5° .

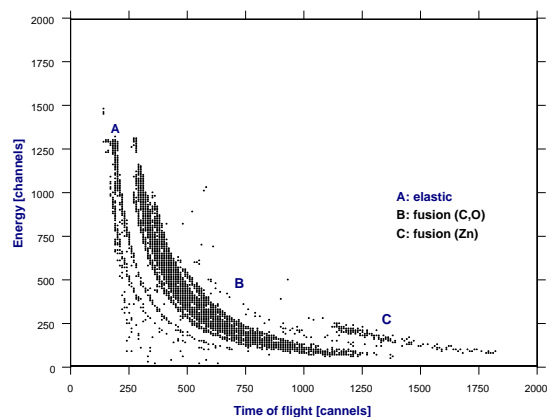


Figure 2. Typical time of flight spectra, for the system ${}^6\text{Li} + {}^{64}\text{Zn}$ at $E_{Lab} = 16$ MeV and $\theta_{Lab} = 12^\circ$.

2 Experimental results

We have performed measurements of angular distributions at scattering angles $\theta_{Lab} = 10^\circ, 12^\circ, 15^\circ$ and 20° at energies of 20 MeV for the ${}^6\text{Li} + {}^{64}\text{Zn}$, ${}^{27}\text{Al}$ systems and at 22 MeV for the ${}^9\text{Be} + {}^{27}\text{Al}$ system. For a fixed scattering angle the incident beam energy was varied for each system to

obtain the excitation functions. Table 1 shows the values of the fusion cross sections obtained in the present work. Fig. 2 shows energy vs. time-of-flight spectra, taken at $E_{Lab} = 16$ MeV and $\theta_{Lab} = 12^\circ$ for ${}^6\text{Li} + {}^{64}\text{Zn}$ system. This spectrum shows that the system was able to separate events differing by one or two units of atomic mass and that the fusion products are well separated relative to the reaction products stemming from the ${}^{12}\text{C}$ target backing and ${}^{16}\text{O}$ target contaminants. The masses of the residual nuclei originating from the complete fusion (CF) and those from the incomplete fusion (ICF) are mostly the same and we were not able to separate the CF from ICF. Therefore, the measured fusion cross sections correspond to the sum of these two processes.

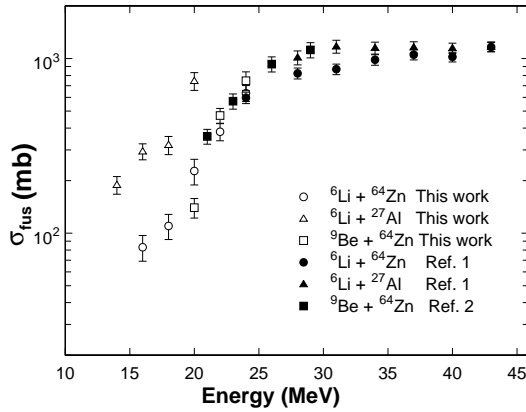


Figure 3. Fusion cross section vs. bombarding energy plot for the data of the Ref. [1], Ref. [2] and the results of this work.

TABLE 1: Results for the total fusion cross sections measured in this work (in mb).

E_{Lab} [MeV]	${}^6\text{Li} + {}^{64}\text{Zn}$	${}^6\text{Li} + {}^{27}\text{Al}$	${}^9\text{Be} + {}^{64}\text{Zn}$
14		288 ± 25	
16	114 ± 13	499 ± 42	
18	145 ± 14	590 ± 50	
20	332 ± 25	741 ± 65	140 ± 18
22	488 ± 41		472 ± 46
24	634 ± 48		747 ± 92

TABLE 2: Total fusion cross sections measured in previous works (in mb).

E_{Lab} [MeV]	${}^6\text{Li} + {}^{64}\text{Zn}$ [1]	${}^6\text{Li} + {}^{27}\text{Al}$ [1]	${}^9\text{Be} + {}^{64}\text{Zn}$ [2]
21			358 ± 36
23			570 ± 57
24	597 ± 45		
26			930 ± 93
28	823 ± 59	1014 ± 93	
29			1121 ± 112
31	869 ± 60	1173 ± 100	
34	984 ± 68	1152 ± 90	
37	1053 ± 71	1162 ± 86	
40	1022 ± 65	1148 ± 78	
43	1166 ± 71	1170 ± 77	

Table 2 shows the previously measured fusion cross sections for the ${}^6\text{Li} + {}^{27}\text{Al}$, ${}^{64}\text{Zn}$ systems [1] and ${}^9\text{Be} + {}^{64}\text{Zn}$ system [2]. The complete set of data are plotted in Fig. 3. The uncertainties for the total fusion cross-sections for the different systems range from 10% to 15%.

The new data for the ${}^6\text{Li} + {}^{27}\text{Al}$ and ${}^6\text{Li} + {}^{64}\text{Zn}$ systems follow the same tendency as the previous one.

The new data will be further investigated and additional experiments will be carried out in the near future in order to complete the three fusion excitation functions discussed here. The comparison with theoretical predictions will be performed.

References

- [1] I. Padron *et al.*, Phys. Rev. C **66**, 044608 (2002).
- [2] S. B. Moraes *et al.*, Phys. Rev. C **61**, 064608 (2000).